

Sensitive Electrochemical Immunosensor for Detection of Mycotoxins Aflatoxin B1 Using Disposable screen-Printed Carbon Electrode

Ping liu, Xingpu Qi, Huanxin Zhang, Yi Zheng*

Jiangsu Agri-animal Husbandry Vocational College, No 8 East Phoenix Road, Taizhou, Jiangsu, 225300, P.R.China

*E-mail: qixingpu@163.com

Received: 1 November 2020/ Accepted: 23 December 2020 / Published: 31 January 2021

This study presented the preparation of sensitive electrochemical immunosensor to detect mycotoxins aflatoxin B1 (AFB1) by immobilization of monoclonal antibodies of AFB1 on disposable screen-printed carbon electrode (SPCE) surface (anti-AFB1/SPCE). The morphological and structural properties of prepared SPCE were studied by XRD and FESEM analysis which showed the carbon structure of SPCE covered the electrode surface with rough and porous morphology. Differential pulse voltammetry (DPV) and Cycle voltammetry (CV) techniques were applied to record the electrochemical responses of anti-AFB1/SPCE and SPCE. CV studies showed the electrochemical responses of anti-AFB1/SPCE were more stable and sensitive toward SPCE in $[\text{Fe}(\text{CN})_6]^{3-/4-}$ as redox probe solution due to the synergistic effect between porous morphology of SPCE and immobilization of anti-AFB1 and its the great electrochemical reaction capability and fast rates of electron transfer on anti-AFB1/SPCE surface. DPV measurements showed the linear range and limit of detection of AFB1 on anti-AFB1/SPCE were obtained 10 to 120 $\text{ng}\cdot\text{ml}^{-1}$ and 0.007 $\text{ng}\cdot\text{ml}^{-1}$, respectively which illustrating the comparable or better electrochemical performance of anti-AFB1/SPCE for determination of AFB1 in comparison with other reported AFB1 immunosensors in literatures. Studying the capability of anti-AFB1/SPCE in a prepared real sample of maize showed the obtained AFB1 concentration in pure real solution was 9.73 $\text{ng}\cdot\text{ml}^{-1}$ that was consistent with the results obtained by high performance liquid chromatography method. Furthermore, results demonstrated the obtained recovery and relative standard deviation values were acceptable and the prepared immunosensor was reliable to determine AFB1 in real samples.

Keywords: Immunosensor; Aflatoxin B1; Cycle voltammetry; Differential pulse voltammetry; Linear range; Limit of detection

1. INTRODUCTION

Aflatoxin B1 (AFB1, $\text{C}_{17}\text{H}_{12}\text{O}_6$) as the predominant mycotoxin and most toxic aflatoxin is one

of main potent carcinogens in foods that prepared by *Aspergillus flavus* and *Aspergillus parasiticus*[1]. AFB1 is found a common pre-harvest and post-harvest contaminant in a variety of human and animals foods such as maize, corn, pistachios, peanuts, cottonseed meal, coffee, rice, spices and oats, rye, wheat, barley, soya, and other cereals and nuts [1-3].

Humans and animals are almost exposed to AFB1 through diet. Furthermore, AFB1 can permeate through the skin. Results show that it plays a major role in causing the types human and animals hepatocellular carcinoma [4, 5]. Moreover, it observed that the AFB1 has been exhibited mutagenic, teratogenic, and led to immunosuppression [2, 4].

Production of AFB1 in foods and food produces is increased in hot and humid climates. Accordingly, the most AFB1 contaminated foods have been reported in Southeast Asia, South America, and Sub-Saharan Africa [6, 7]. Therefore, several countries determine rules and regulations governing AFB1 in foods to the limitation of AFB1 levels in food products. For example, United States food safety regulations have limited the AFB1 level up to 20 $\mu\text{g}/\text{kg}$ in foods [8, 9]. European Union has also limited the permitted level of AFB1 2 to 12 $\mu\text{g}/\text{kg}$ in adult foods, 0.1 $\mu\text{g}/\text{kg}$ in infant foods and 5-50 $\mu\text{g}/\text{kg}$ in animal feeds [10, 11]. FAO has set the maximum permitted levels of AFB1 to be 10 and 15 $\mu\text{g}/\text{kg}$ in processed and raw peanuts, respectively.

Thus, determination of AFB1 by analytical methods is important and many researches have been conducted to optimize sensing properties of sensor and immunosensors of AFB1. Thin-layer chromatography (TLC), high-performance liquid chromatography (HPLC), high-performance liquid chromatography-fluorescence (HPLC-FL), liquid chromatography–tandem mass spectrometry (LC–MS/MS), mass spectrometry, fluorometry, enzyme-linked immunosorbent assay (ELISA) and electrochemistry are the common analytical methods for determination of AFB1 in food samples [12-15]. Among them, many studies have been performed using the electrochemical techniques such as electrochemical impedance spectroscopy, CV and DPV because of their low cost, fast response and simplicity for AFB1 determination [16-19]. Furthermore, modification of electrodes and bioelectrodes electrochemical techniques can provide the capability for increasing the sensitivity, linear range and detection limit of sensor and immunosensors. For example, Li et al. [20] applied thionine-graphene nanocomposite and ferrocene-labeled aptamer to output current signals to electrochemical determination of AFB1 and showed great accuracy and reliability compared with the HPLC-FL as an official method. Tan et al. constructed a sensitive and simple electrochemical immunosensor based on enzymatic silver deposition amplification to determine AFB1 in spiked rice samples [21-23] and showed the good capability of proposed immunosensor for monitoring AFB1 in real samples.

Therefore, this study revealed the preparation, characterization and application of electrochemical immunosensor of AFB1 based on immobilization of monoclonal antibodies of AFB1 on SPCE surface.

2. EXPERIMENTAL

2.1. Preparation of SPCE and anti-AFB1/SPCE

The SPCE was prepared using carbon conductive inks (Foshan Yinya Technology Company limited, China) and was printed through a patterned (1 mm thick) on polypropylene (PP, Foshan Guide Textile Co., Ltd., China) base. Then, SPCE was cured for one hour at 90 °C. There were working

areas of 750.3 mm and strips of 1650.5 mm for prepared SPCE. For activation of the functional groups of electrode, the SPCE was treated with cross-linked solution for 5 hours which containing 0.3 M 1-ethyl-3-(3-dimethylaminopropyl)carbodiimide (EDC, Sigma-Aldrich, UK) as coupling agent and 0.06 M N-hydroxysuccinimide (NHS, Sigma-Aldrich, UK) as activator agent. After that, the SPCE was immersed in 0.2 gl^{-1} monoclonal antibodies of AFB1 (anti-AFB1, Sigma-Aldrich, UK) for 24 hours at room temperature. After that, the immersed electrode was rinsed with deionized water and transferred to the refrigerator 5 °C for electrochemical studies.

2.2. Measurement and analyses techniques

The field emissionscanning electron microscopy (FESEM; SU5000, Hitachi High-Technologies Corporation, Tokyo, Japan) and X-ray diffraction (XRD) with $\text{CuK}\alpha$ radiation source ($\lambda = 1.540 \text{ \AA}$) were used for study of morphology and crystal structures of prepared electrodes. CV and DPV measurements were done by AUTOLAB electrochemical system (Metrohm Autolab B.V., The Netherlands) in three-electrode electrochemical cell which contained Ag/AgCl as reference, Pt as counter and the prepared electrode (SPCE and anti-AFB1/SPCE) as working electrodes. The electrochemical CV and DPV studies were recorded in 0.1 M phosphate buffer solutions (PBS) containing 2mM $[\text{Fe}(\text{CN})_6]^{3-/4-}$ (99%, Haihang Industry Co.,Ltd., China). PBS was prepared from 0.1 M H_3PO_4 (85%, Liuzhou Xianmi Trade Co., Ltd., China) and 0.1 M NaH_2PO_4 (98%, Sichuan Kindia May Science And Tech Co., Ltd., China) and its pH was adjusted with HCl (34%, Zhengzhou Qiangjin Science And Technology Trading Co., Ltd., China) and NaOH (99%, Tianjin City Jinhongweibang Chemical Co., Ltd., China) solutions.

2.3. Preparation the real sample

In order to prepare the real sample, 100 mg of pure maize powder was ultrasonically added to a 15 ml mixture solution of 0.1 M PBS and methanol (1:9 v:v) and transferred to the refrigerator at 10°C for 24 hours. The resulting mixture was centrifuged at 2500 rpm for 15 minutes and filtered. Ultimately, 10 ml of supernatant was used as the real sample.

3. RESULTS AND DISCUSSION

3.1. Structural analysis of SPCE

In order to study the structure of SPCE, its XRD and FESEM analyses are presented in Figure 1a and 1b, respectively. As seen in Figure 1a, there is a diffraction at $2\theta = 26.95^\circ$ which corresponds to formation (002) of carbon structure [24]. The morphology of electrode surfaces is shown in Figure 1b. As observed, the big grains of carbon covered the electrode surface which formed a rough and porous morphology.

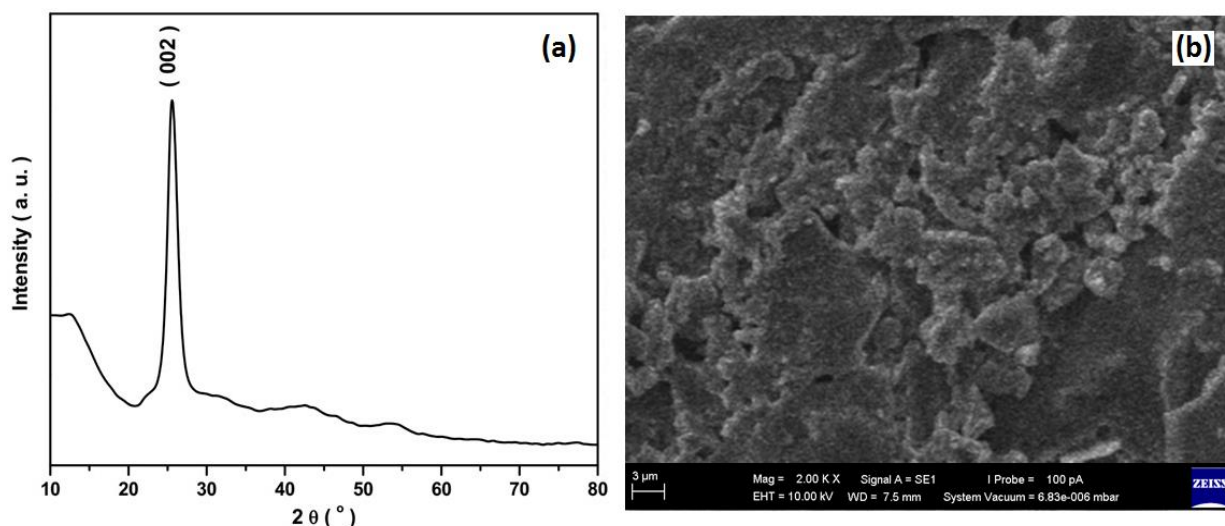


Figure 1. (a) XRD and (b) FESEM analysis of SPCE

3.2. Electrochemical study of anti-AFB1/SPCE

CV and DPV techniques were conducted to electrochemical characterization of SPCE and anti-AFB1/SPCE.

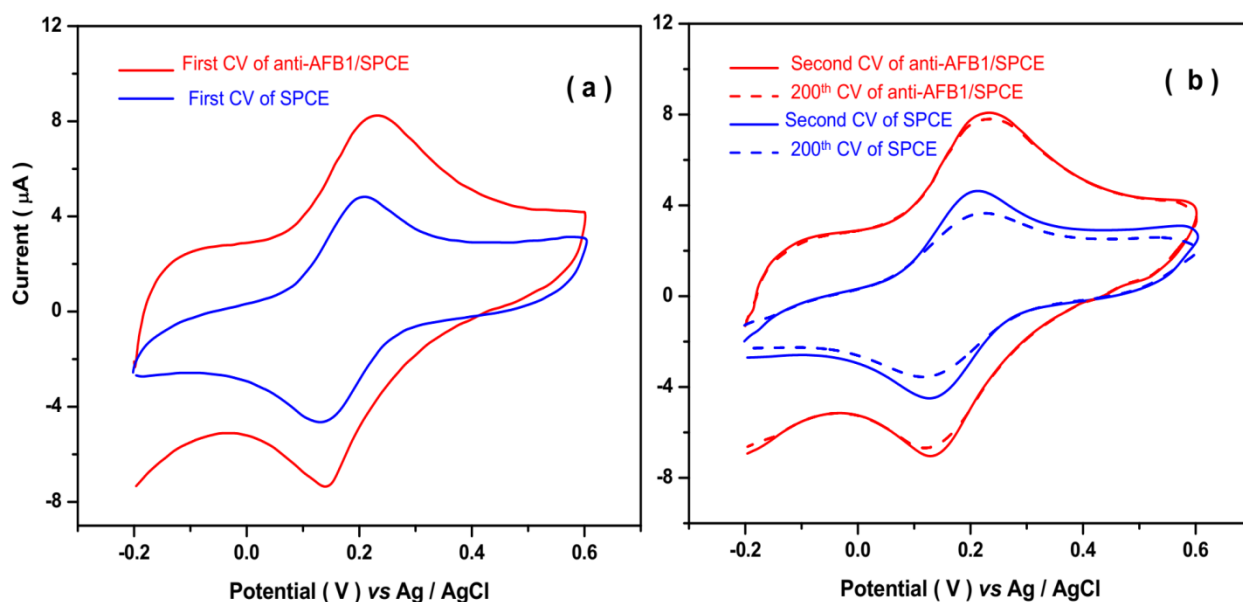


Figure 2. (a) The first, (b) second and 200th recorded CVs of SPCE and anti-AFB1/SPCE under applied potential range from -0.2 to 0.6 V at 50 mVs⁻¹ in 0.1M PBS solution pH 7.1 containing 2mM [Fe(CN)₆]^{3-/4-}.

The recorded CVs are shown in Figure 2 to study the interaction between biomolecules and the electrode surface under applied potential range from -0.2V to 0.6V at 10 mV s⁻¹ in 0.1M PBS solution

pH 7.1 containing 2 mM $[\text{Fe}(\text{CN})_6]^{3-/4-}$ as redox probe solution. The recorded anodic and cathodic peaks current of SPCE are observed of 4.78 μA and -4.66 μA at potential of 0.19 V and 0.13 V, respectively. The recorded anodic and cathodic peaks current of anti-AFB1/SPCE are observed of 8.25 μA and -7.38 μA at potential of 0.23 V and 0.14 V, respectively. As shown in Fig.2a, the current response of anti-AFB1/SPCE is increased which may be due to the synergistic effect between porous morphology of SPCE and immobilization of anti-AFB1 [25, 26]. Figure 2b shows the stability effect of SPCE and anti-AFB1/SPCE with record of successive CVs. It is observed that comparison between the second and 200th recorded CVs responses of SPCE and anti-AFB1/SPCE reveals 25.8% and 6.2% changes for redox peak currents that show the more stability response of anti-AFB1/SPCE. Therefore, further electrochemical studies were conducted on anti-AFB1/SPCE.

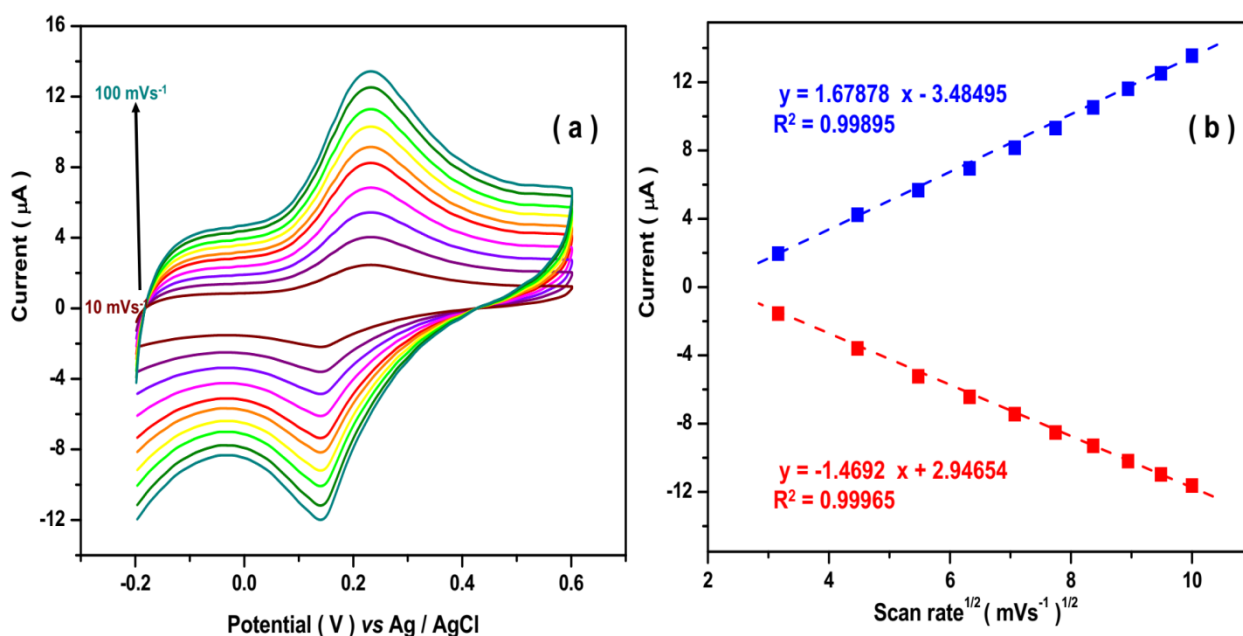


Figure 3. (a) The recorded CVs of anti-AFB1/SPCE at various scan rates from 10 mV s^{-1} to 100 mV s^{-1} under applied potential range from -0.2V to 0.6V in 0.1 M PBS solution pH 7.1 containing 2mM $[\text{Fe}(\text{CN})_6]^{3-/4-}$. (b) Redox peak currents vs. square root of the scan rate.

Figure 3a shows the recorded CVs of anti-AFB1/SPCE for electrochemical scan rate effect at different scan rates from 10 mV s^{-1} to 100 mV s^{-1} which indicated the peak potential values are expanded towards the positive as well as negative direction with increasing the scan rate value. It implies the efficient mass transfer on the electrode surface [27, 28]. Furthermore, the redox peak currents are linearly increased by increasing the scan rate value (Figure 3b). The linear relationship between peak current values with the square-root of scan rate in Figure 3b shows that the redox reaction is controlled through the quasi-reversible diffusion process on the electrode surface [29]. Moreover, the electrochemical scan rate effect demonstrates the great electrochemical reaction capability and fast rates of electron transfer on anti-AFB1/SPCE surface [29, 30]. The intensity of peak current density depends on the electroactive surface area ($A(\text{cm}^2)$) and the density of electroactive catalytically species ($C(\text{mol}/\text{cm}^3)$) on electrode are the main effective parameters on peak current density ($I_p(\text{A})$) which can be described by Randles-Sevcik equation as following formula (1) [31, 32]:

$$I_p = 2.69 \times 10^5 n^{3/2} AD^{1/2} C v^{1/2} \quad (1)$$

Where n shows the number of electrons transferred in the redox event ($n = 1$), D (cm^2s^{-1}) is diffusion coefficient of $[\text{Fe}(\text{CN})_6]^{3-/4-}$ ($6.5 \times 10^{-6} \text{ cm}^2 \text{ s}^{-1}$) [33, 34] and v is the scan rate (Vs^{-1}). Therefore, the effective surface area can be obtained of $1.52 \times 10^{-5} \text{ cm}^2$ for anti-AFB1/SPCE from slope of anodic peak current vs $v^{1/2}$.

3.3. Electrochemical response of anti-AFB1/SPCE to addition AFB1

The electrochemical response of anti-AFB1/SPCE was studied toward various concentration of AFB1 through record the CVs in potential range from -0.2 to 0.6 V at 50 mVs^{-1} in 0.1 M PBS solution pH 7.1 containing 2 mM $[\text{Fe}(\text{CN})_6]^{3-/4-}$. Fig. 4 shows that the current response of anodic peak linearly increases with additions of 0.5 , 1 and 1.5 ng ml^{-1} solution of AFB1 in electrochemical cells which indicates the high sensitive response of electrodes to addition of AFB1. The enhancement of signal may be related to electrochemical interaction between AFB1 and anti-AFB1 on electrode surfaces [35, 36]. Moreover, it can be attributed to form the electron transfer substrate [37].

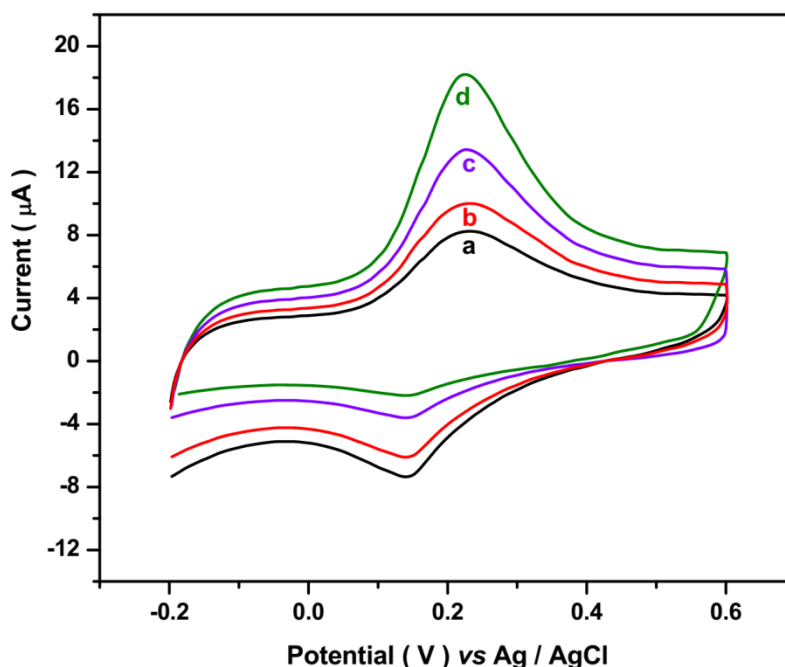


Figure 4. The recorded CVs of anti-AFB1/SPCE to addition of (a) 0(b) 0.5(c) 1 and (d) 1.5 ng ml^{-1} AFB1 solution in electrochemical cell under applied potential range from -0.2 V to 0.6 V at scan rates of 10 mV s^{-1} in 0.1 M PBS solution pH 7.1 containing 2 mM $[\text{Fe}(\text{CN})_6]^{3-/4-}$.

Further, electrochemical studies were done by DPV technique for determination the sensing properties of anti-AFB1/SPCE toward addition AFB1 solution in potential range from -0.2 V to 0.6 V at 50 mVs^{-1} in 0.1 M PBS solution pH 7.1 containing 2 mM $[\text{Fe}(\text{CN})_6]^{3-/4-}$.

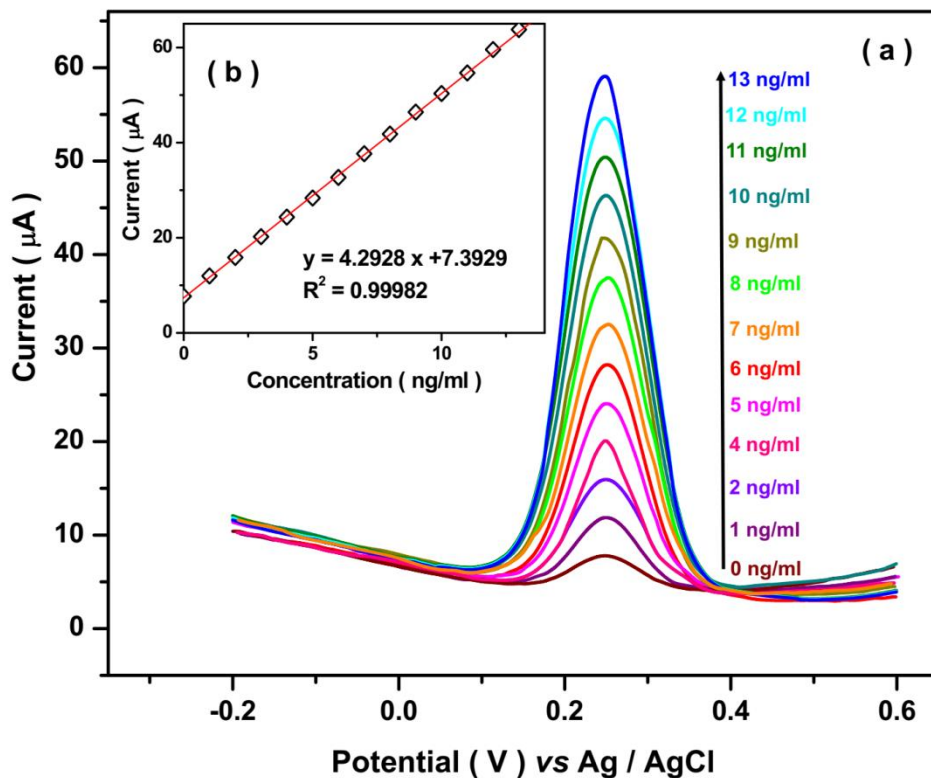


Figure 5. (a) The electrochemical DPV response and (b) calibration plot of anti-AFB1/SPCE to successive addition of 1 ng ml⁻¹ AFB1 solution in potential range from -0.2V to 0.6V at 50 mVs⁻¹ in 0.1 M PBS solution pH 7.1 containing 2mM [Fe(CN)₆]^{3-/4-}.

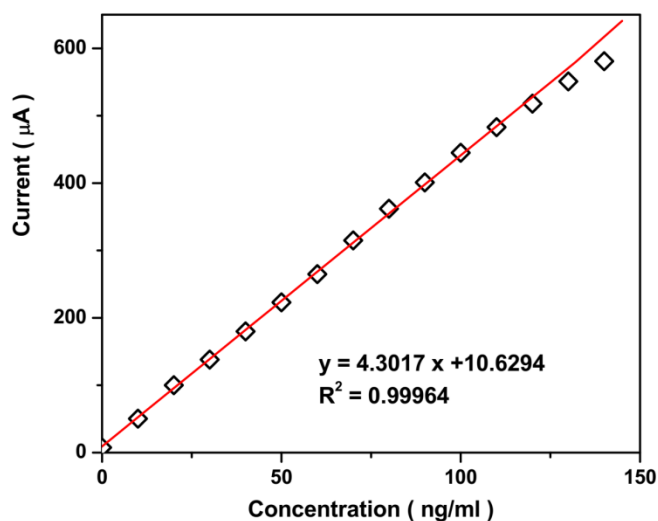


Figure 6. The calibration plot of anti-AFB1/SPCE for successive addition of 10 ng ml⁻¹ AFB1 solution in potential range from -0.2V to 0.6V at 50 mVs⁻¹ in 0.1M PBS solution pH 7.1 containing 2mM [Fe(CN)₆]^{3-/4-}.

Figures 5a and 5b exhibit the electrochemical DPV response and calibration plot of electrode to successive addition of 1 ng ml⁻¹ AFB1 solution which evidence to the linear response of electrode to addition of analyte. The limit of detection of AFB1 on anti-AFB1/SPCE is achieved 0.007 ng ml⁻¹. For

determination of the maximum linear range of immunosensor, the DPV measurement was performed for successive injection of 10 ng ml⁻¹ AFB1 solution as high concentration addition of analyte solution. The obtained calibration plot in Figure 6 shows that the linear range for detection of AFB1 on anti-AFB1/SPCE was achieved 10 to 120 ng ml⁻¹. The resulted sensing properties of anti-AFB1/SPCE are compared with other reported AFB1 sensor immunosensors in literatures in Table 1 which indicating the anti-AFB1/SPCE shows the comparable electrochemical properties and wide linear range for determination of AFB1 due to high porosity of substrate that provides high effective surface area for immobilization of biomolecules [31].

Table 1. Comparison between the resulting sensing properties of anti-AFB1/SPCE with other reported AFB1 sensors in literature.

Immunosensor	Technique	Limit of detection (ng/ml)	Detection range (ng/ml)	Ref.
Anti-AFB1/SPCE	DPV	0.007	10-120	This work
Polythionine /Au/glassy carbon electrode	DPV	0.07	0.6–2.4	[38]
Poly (3,4-ethylenedioxythiophene)/AuNPs/ITO	CV	0.004	1–25	[39]
96-well screen printed microplate	IPA*	0.03	0.05- 2	[40]
carboxylated MWCNTs/ITO electrode	CV	0.08	0.25–1.375	[41]
graphene quantum dots -AuNPs/ITO	CV	0.008	0.1–3.0	[42]

*Intermittent pulse amperometry

In order to examine the capability of prepared immunosensor in real sample, the DPV technique was applied with addition of the 1 ng ml⁻¹ of AFB1 in electrochemical cell containing 10 ml of 0.1M PBS solution pH 7.1 containing 2mM [Fe(CN)₆]^{3-/4-} and 10 ml of prepared real sample of maize under potential range from -0.2V to 0.6V at 50 mVs⁻¹. The DPV response and its calibration plot in Figure 7 show that the AFB1 concentration in pure real solution was obtained 4.86 ng ml⁻¹ in electrochemical cell and 9.73 ng ml⁻¹ in prepared real sample which is consistent with the results obtained by high performance liquid chromatography method with Triple Quadrupole Tandem mass spectrometry detector [43]. Furthermore, analytical applicability of the anti-AFB1/SPCE was also studied to determine AFB1 in real samples. Table 2 shows the obtained recovery (RE) and RSD values are acceptable and the prepared immunosensor is reliable for the determination of AFB1 in real samples.

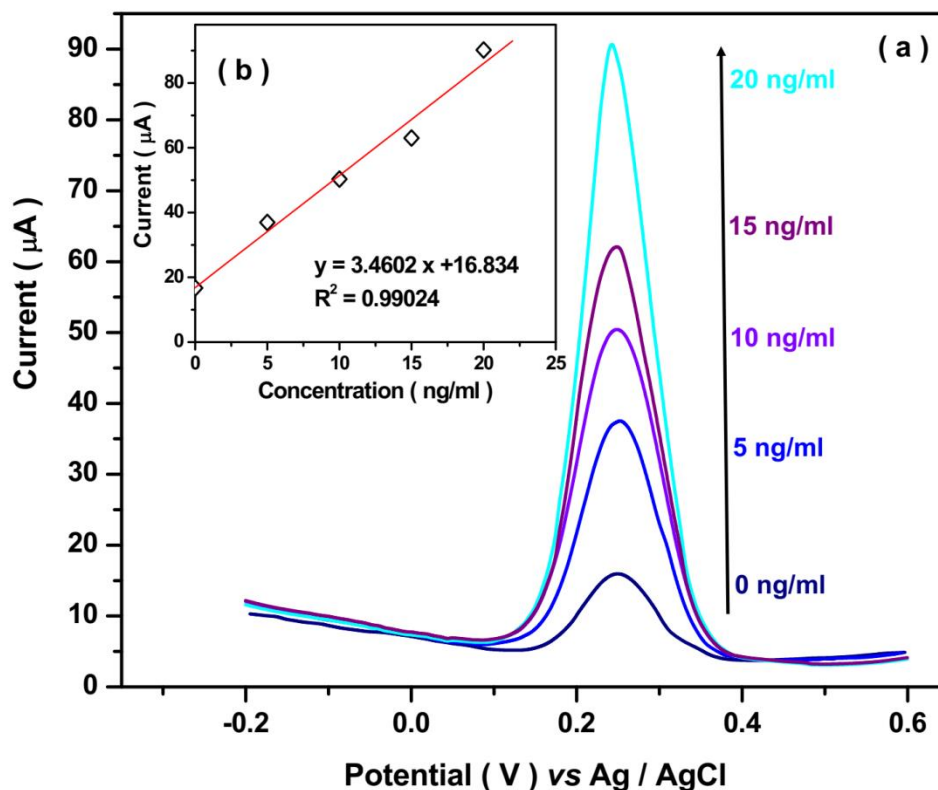


Figure 6. (a) The DPV response and (b) the calibration plot of anti-AFB1/SPCE for addition of the prepared real samples solution in potential range from -0.2V to 0.6V at 50 mVs^{-1} in 0.1M PBS solution pH 7.1 containing $2\text{mM } [\text{Fe}(\text{CN})_6]^{3-/4-}$.

Table 2. Analytical results to determination of AFB1 in real samples.

Sample	Added (μM)	Measured (μM)	RE (%)	RSD (%)
Maize	5.00	4.93	98.6	3.14
	10.00	9.68	96.8	2.74
	15.00	13.33	88.8	4.50
	20.00	18.65	93.2	4.05

4. CONCLUSION

This study was conducted for preparation of a sensitive electrochemical immunosensor to detect mycotoxins aflatoxin B1 using SPCE. The immunosensor was prepared by immobilization of monoclonal antibodies of AFB1 on SPCE surface. XRD and FESEM analyses were applied for study of the structure and morphology of prepared SPCE which exhibited the carbon structure of SPCE covered the electrode surface with rough and porous morphology. CV and DPV measurements were performed for the electrochemical analyses. CV measurements showed the electrochemical responses of anti-AFB1/SPCE were more stable and sensitive toward SPCE in $[\text{Fe}(\text{CN})_6]^{3-/4-}$ as redox probe

solution due to the synergistic effect between porous morphology of SPCE and immobilization of anti-AFB1 and the great electrochemical reaction capability and fast rates of electron transfer on anti-AFB1/SPCE surface. DPV measurements showed the linear range and limit of detection of AFB1 on anti-AFB1/SPCE were achieved 10 to 120ng ml⁻¹ and 0.007ng ml⁻¹, respectively. The resulting sensing properties of anti-AFB1/SPCE were compared with other reported AFB1 immunosensors in literature which indicated the anti-AFB1/SPCE had the comparable electrochemical performance and wide linear range for determination of AFB1. The capability of anti-AFB1/SPCE was examined in a prepared real sample of maize which implying the obtained AFB1 concentration in pure real solution was 9.73 ng ml⁻¹ that it was consistent with the results obtained by high performance liquid chromatography method. Moreover, results exhibited the obtained recovery and RSD values were acceptable and the prepared immunosensor was reliable to determine AFB1 in real samples.

ACKNOWLEDGEMENT

This work was supported by TaiZhou 311 Project, and Detection of mycotoxin residues in live and slaughtered products of waterfowl ,Number:NSFKF201905

References

1. A.M. Fouad, D. Ruan, H.K. El-Senousey, W. Chen, S. Jiang and C. Zheng, *Toxins*, 11(2019)176.
2. L. Afsah-Hejri, S. Jinap, P. Hajeb, S. Radu and S. Shakibazadeh, *Comprehensive Reviews in Food Science and Food Safety*, 12(2013)629.
3. H. Karimi-Maleh and O.A. Arotiba, *Journal of colloid and interface science*, 560(2020)208.
4. M.E. Smela, M.L. Hamm, P.T. Henderson, C.M. Harris, T.M. Harris and J.M. Essigmann, *Proceedings of the National Academy of Sciences*, 99(2002)6655.
5. J. Rouhi, C.R. Ooi, S. Mahmud and M.R. Mahmood, *Materials Letters*, 147(2015)34.
6. C.P. Wild and R. Montesano, *Cancer letters*, 286(2009)22.
7. H. Karimi-Maleh, F. Karimi, M. Alizadeh and A.L. Sanati, *The Chemical Record*, 20(2020)682.
8. D.L. Park and B. Liang, *Trends in Food Science & Technology*, 4(1993)334.
9. R. Dalvand, S. Mahmud, J. Rouhi and C.R. Ooi, *Materials Letters*, 146(2015)65.
10. A. Ouakhsase, A. Chahid, H. Choubbane, A. Aitmazirt and E.A. Addi, *Heliyon*, 5(2019)e01565.
11. A. Khodadadi, E. Faghih-Mirzaei, H. Karimi-Maleh, A. Abbaspourrad, S. Agarwal and V.K. Gupta, *Sensors and actuators b: chemical*, 284(2019)568.
12. Z. Han, Y. Ren, J. Zhu, Z. Cai, Y. Chen, L. Luan and Y. Wu, *Journal of Agricultural and food Chemistry*, 60(2012)
13. H. Zhang, Z. Shi, S. Cheng, Q. Yang, X. Sun and Y. Guo, *International Journal of Electrochemical Science*, 14(2019)9170.
14. A. Fan, L. Shi, H. Yang and G. Yang, *International Journal of Electrochemical Science*, 15(2020)9669.
15. S. Changaei, J. Zamir-Anvari, N.-S. Heydari, S.G. Zamharir, M. Arshadi, B. Bahrami, J. Rouhi and R. Karimzadeh, *Journal of Electronic Materials*, 48(2019)6216.
16. S. Feng, J. Meng, J. Guo, X. Chen, G. Zhang, W. Liu, G. Liu, G. Yang and H. Sun, *International Journal of Electrochemical Science*, 15(2020)7722.
17. X. Chen, H. Li, G. Zhang, S. Feng, G. Yang, L. Shi, W. Liu, L. Guiyang and H. Pan, *International Journal of Electrochemical Science*, 15(2020)6269.

18. J. Rouhi, C.R. Ooi, S. Mahmud and M.R. Mahmood, *Electronic Materials Letters*, 11(2015)957.
19. J. Rouhi, S. Mahmud, S.D. Hutagalung, N. Naderi, S. Kakooei and M.J. Abdullah, *Semiconductor Science and Technology*, 27(2012)065001.
20. Y. Li, D. Liu, C. Zhu, M. Wang, Y. Liu and T. You, *Sensors and Actuators B: Chemical*, (2020)129021.
21. Y. Tan, X. Chu, G.-L. Shen and R.-Q. Yu, *Analytical Biochemistry*, 387(2009)82.
22. Z. Shamsadin-Azad, M.A. Taher, S. Cheraghi and H. Karimi-Maleh, *Journal of Food Measurement and Characterization*, 13(2019)1781.
23. M. Alimanesh, J. Rouhi and Z. Hassan, *Ceramics International*, 42(2016)5136.
24. T. Batakliiev, I. Petrova-Doycheva, V. Angelov, V. Georgiev, E. Ivanov, R. Kotsilkova, M. Casa, C. Cirillo, R. Adami and M. Sarno, *Applied Sciences*, 9(2019)469.
25. V. Gascón, I. Díaz, C. Márquez-Álvarez and R.M. Blanco, *Molecules*, 19(2014)7057.
26. F. Tahernejad-Javazmi, M. Shabani-Nooshabadi and H. Karimi-Maleh, *Composites Part B: Engineering*, 172(2019)666.
27. A.A. Bojang and H.S. Wu, *Catalysts*, 10(2020)782.
28. J. Rouhi, S. Kakooei, M.C. Ismail, R. Karimzadeh and M.R. Mahmood, *International Journal of Electrochemical Science*, 12(2017)9933.
29. J.-j. Wu, W.-t. Wang, M. Wang, H. Liu and H.-c. Pan, *International Journal of Electrochemical Science*, 11(2016)5165.
30. J. Rouhi, M.R. Mahmood, S. Mahmud and R. Dalvand, *Journal of Solid State Electrochemistry*, 18(2014)1695.
31. Z. Savari, S. Soltanian, A. Noorbakhsh, A. Salimi, M. Najafi and P. Servati, *Sensors and Actuators B: Chemical*, 176(2013)335.
32. M. Zaib and M.M. Athar, *International Journal of Electrochemical Science*, 10(2015)6690.
33. C.S.R. Vusa, V. Manju, S. Berchmans and P. Arumugam, *RSC advances*, 6(2016)33409.
34. H. Karimi-Maleh, K. Cellat, K. Arıkan, A. Savk, F. Karimi and F. Şen, *Materials Chemistry and Physics*, 250(2020)123042.
35. C. Wang and Q. Zhao, *Analytical and bioanalytical chemistry*, 411(2019)6637.
36. Z. Zhuang, Y. Huang, Y. Yang and S. Wang, *Journal of hazardous materials*, 301(2016)297.
37. D. Feng, X. Lu, X. Dong, Y. Ling and Y. Zhang, *Microchimica Acta*, 180(2013)767.
38. J.H. Owino, O.A. Arotiba, N. Hendricks, E.A. Songa, N. Jahed, T.T. Waryo, R.F. Ngece, P.G. Baker and E.I. Iwuoha, *Sensors*, 8(2008)8262.
39. A. Sharma, A. Kumar and R. Khan, *Materials Science and Engineering: C*, 76(2017)
40. S. Piermarini, L. Micheli, N. Ammida, G. Palleschi and D. Moscone, *Biosensors and Bioelectronics*, 22(2007)1434.
41. C. Singh, S. Srivastava, M.A. Ali, T.K. Gupta, G. Sumana, A. Srivastava, R. Mathur and B.D. Malhotra, *Sensors and Actuators B: Chemical*, 185(2013)258.
42. H. Bhardwaj, M.K. Pandey and G. Sumana, *Microchimica Acta*, 186(2019)592.
43. L. de Almeida, R. Williams, D.M. Soares, H. Nesbitt, G. Wright and W. Erskine, *Scientific reports*, 9(2019)1.